Assessment of mitochondrial energy coupling *in vivo* by $^{13}C/^{31}P$ NMR

Beat M. Jucker*, Sylvie Dufour†, Jianming Ren*‡, Xueying Cao‡, Stephen F. Previs*, Brian Underhill*, Kevin S. Cadman*, and Gerald I. Shulman*†§¶

Departments of *Internal Medicine and ¶Cellular and Molecular Physiology, and †Howard Hughes Medical Institute, Yale University School of Medicine, P.O. Box 9812, New Haven, CT 06510; and ‡Department of Metabolic Research Bristol-Myers Squibb, Princeton, NJ 08543

Communicated by David M. Kipnis, Washington University School of Medicine, St. Louis, MO, March 23, 2000 (received for review February 2, 2000)

The recently cloned uncoupling protein homolog UCP3 is expressed primarily in muscle and therefore may play a significant role in the regulation of energy expenditure and body weight. However, investigation into the regulation of uncoupling protein has been hampered by the inability to assess its activity *in vivo*. In this report, we demonstrate the use of a noninvasive NMR technique to assess mitochondrial energy uncoupling in skeletal muscle of awake rats by combining ^{13}C NMR to measure rates of mitochondrial substrate oxidation with ^{31}P NMR to assess unidirectional ATP synthesis flux. These combined $^{31}P/^{13}C$ NMR measurements were performed in control, 10-day triiodo-L-thyronine (T_3)-treated (model of increased UCP3 expression), and acute 2,4-dinitrophenol (DNP)-treated (protonophore and mitochondrial uncoupler) rats. UCP3 mRNA and protein levels increased 8.1-fold (± 1.1) and 2.8-fold (± 0.8), respectively, in the T_3-treated vs. control rat gastrocnemius muscle. ^{13}C NMR measurements of tricarboxylic acid cycle flux as an index of mitochondrial substrate oxidation were 61 ± 21, 148 ± 25, and 310 ± 48 nmol/g per min in the control, T_3, and DNP groups, respectively. ^{31}P NMR saturation transfer measurements of unidirectional ATP synthesis flux were 83 ± 14, 84 ± 14, and 73 ± 7 nmol/g per s in the control, T_3, and DNP groups, respectively. Together, these flux measurements, when normalized to the control group, suggest that acute administration of DNP (mitochondrial uncoupler) and chronic administration of T_3 decrease energy coupling by ≈80% and ≈60%, respectively, and that the latter treatment correlates with an increase in UCP3 mRNA and protein expression. This NMR approach could prove useful for exploring the regulation of uncoupling protein activity *in vivo* and elucidating its role in energy metabolism and obesity.

Mitochondrial uncoupling proteins (UCP) play an integral role in regulating cellular energy consumption via nonshivering thermogenesis (1). This regulation is accomplished by diminishing the proton motive force across the inner mitochondrial membrane, which results in uncoupling of respiration from ATP synthesis. Unlike UCP1, which is expressed exclusively in brown adipose tissue, the recently discovered homolog UCP3 (2, 3) is expressed primarily in muscle and is encoded in a chromosomal region linked to hyperinsulinemia and obesity (4). Because quiescent skeletal muscle accounts for 33% of whole-body oxygen consumption (5), much attention has been given to the control and function of UCP3 as a means of regulating energy expenditure and body weight. However, investigation into the regulation of uncoupling protein has been hampered by the inability to assess its activity in intact tissue. In this report, we present a method of assessing mitochondrial energy coupling noninvasively in skeletal muscle by combining ^{13}C NMR spectroscopy to measure rates of mitochondrial substrate oxidation with ^{31}P NMR spectroscopy to assess rates of unidirectional ATP synthesis in (*i*) awake control rats, (*ii*) chronic triiodo-L-thyronine (T_3)-treated rats (a model of increased thermogenesis and UCP3 expression), and (*iii*) acute 2,4-dinitrophenol (DNP)-treated (protonophore and mitochondrial uncoupler) rats. Although this *in vivo* NMR technique cannot be used to measure explicit uncoupling protein function *per se*, it can be used to measure a decrease in mitochondrial energy coupling resulting from increased uncoupling protein function and/or other thermogenic processes.

Materials and Methods

Animals. Sprague–Dawley rats (Charles River Breeding Laboratories) were housed individually in an environmentally controlled room with a 12-h light/12-h dark cycle and maintained on standard rat chow (Purina). Three groups of rats were used: (*i*) control rats (n = 10), (*ii*) T_3-treated rats (n = 10), and (*iii*) DNP-treated rats (n = 9). The T_3 group, when weighing 300–350 g, had cannulas inserted into both the right jugular vein and carotid artery and were allowed to recuperate for 5 days before treatment. Once at preoperative weight, the T_3-treated rats were given 3.5 mg of T_3 (Sigma) dissolved in 300 μl of 0.1 M NaOH per liter drinking water for 8–10 days (6). These rats did not gain weight during the treatment period, although they consumed amounts of food similar the amounts consumed by control rats. When weighing 300–350 g, the control and acute DNP-treated rats were cannulated and allowed to return to preoperative weight. The DNP-treated group received an arterial bolus administration of DNP (4 mg/kg; Sigma). The DNP was dissolved in saline (1 mg/333 μl), adjusted to pH 7, and infused over 15 min before commencement of the NMR experiment.

***In Vivo* NMR Spectroscopy.** On the day of the NMR experiment, fed rats were placed in a customized restraining tube that allowed their left hindlimb to be secured to the outside of the tube in a manner that limited free movement of the leg to facilitate NMR measurements.

The 2-^{13}C acetate (sodium salt; 99% ^{13}C enriched; Cambridge Isotope Laboratories, Cambridge, MA) infusion consisted of a bolus (50 mg/kg body weight) for 1 min followed by a 72 μmol/kg per min continuous infusion. Blood samples were drawn during the baseline NMR measurement at 7.5 min, 15 min, and every 15 min thereafter to assess the 2-^{13}C acetate enrichment time course.

All *in vivo* NMR experiments were performed on a Bruker (Billerica, MA) Biospec 7.0T system (horizontal/22-cm-diameter bore magnet). Both ^{13}C observed/^{1}H decoupled and ^{31}P observed NMR spectroscopy were performed by using concentric surface coils; the outer ^{1}H coil (30 mm) was tuned to 300.54 MHz, and the inner dual frequency ^{13}C or ^{31}P coil (18 mm) was tuned to 75.59 or 121.66 MHz, respectively. The rat

Abbreviations: T_3, triiodo-L-thyronine; DNP, 2,4-dinitrophenol; TCA, tricarboxylic acid; ATP_{ase}, ATP synthase; P_i, inorganic phosphate; GAPDH, glyceraldehyde-3-phosphate dehydrogenase; GAP, glyceraldehyde-3-phosphate; PGK, phosphoglycerate kinase.

§To whom reprint requests should be addressed. E-mail: gerald.shulman@yale.edu.

The publication costs of this article were defrayed in part by page charge payment. This article must therefore be hereby marked "*advertisement*" in accordance with 18 U.S.C. §1734 solely to indicate this fact.

Article published online before print: *Proc. Natl. Acad. Sci. USA*, 10.1073/pnas.120131997. Article and publication date are at www.pnas.org/cgi/doi/10.1073/pnas.120131997

hindlimb was positioned over the $^{13}C/^{31}P$ coil (vertical in plane) and placed in the magnet isocenter.

^{1}H decoupled-^{13}C NMR spectroscopy was performed in the following manner. An initial frequency selective sinc pulse (20 ms) set on the high-field side of the lipid methylene carbon resonance at 30 ppm was followed immediately by a nonselective hard pulse (≈70° flip angle; 5 mm from surface coil). The sinc pulse power was adjusted to eliminate most of the lipid signal in that region. Broadband ^{1}H Waltz-16 decoupling was applied during acquisition, and additional nuclear Overhauser effect was achieved by using low-power decoupling (0.4 W) during the relaxation delay (TR = 0.5 s, NS = 1,800, SW = 20 kHz, 4K data). A 15-min baseline spectrum was followed by subsequent 15-min acquisitions throughout the duration of the experiment.

^{31}P NMR spectroscopy was performed in the following manner. In the saturation transfer experiment, a continuous wave radio frequency pulse was used to saturate the γ-ATP resonance. In the spectrum without γ-ATP saturation, the continuous wave pulse frequency was placed symmetrically to the down-field side of inorganic phosphate (P_i). Both spectra were acquired with a nonselective 90° pulse (TR = 4.4 s, NS = 128, SW = 20 kHz, 4K data). An adiabatic half passage (180°) pulse was used to invert all P_i spins in the inhomogeneous volume of the surface coil (TR = 6.0 s, NS = 64, SW = 20 kHz, 4K data) in the inversion recovery experiment. The six variable delay lengths used in the inversion recovery experiment ranged from 10 ms to 6 s.

All spectra were processed off-line with NUTS NMR processing software (Acorn NMR, Fremont, CA) with peak-fitting capabilities. Baseline subtracted ^{13}C NMR and ^{31}P NMR spectra were processed by using Gaussian filtering and a Gaussian weighted peak-fitting algorithm or peak integration.

ATP Synthase (ATP_{ase}) Activity and Coupled Glyceraldehyde-3-Phosphate Dehydrogenase (GAPDH) and Phosphoglycerate Kinase (PGK) Exchange Measurements. Skeletal muscle from control and T_3-treated rats was removed quickly and washed with cold (1°C) buffer A (250 mM sucrose/1 mM EDTA/50 mM Tris·HCl, pH 7.5). The tissues were cut into small pieces and homogenized in 20 volumes of buffer A. A small portion was homogenized each time with a motor-driven Teflon pestle. The homogenate was centrifuged at 1,500 rpm for 3 min and then at 1,700 rpm for 5 min in the Beckman–Coulter J2-MI centrifuge. The supernatant was centrifuged at 10,000 rpm for 17 min. The pellets were resuspended in buffer B (250 mM sucrose/1 mM EDTA/10 mM Tris·HCl, pH 7.4).

ATP_{ase} activity was assayed with a spectrophotometer monitoring the increase in absorbance at 340 nm by using a NADP-linked ADP-regenerating system. Aliquots of isolated mitochondria were added to the reaction medium containing 400 mM glucose, 100 mM $MgCl_2$, 100 mM KPO_4, 200 mM potassium succinate, 110 mM AMP, 10 mM Hepes, 7.5 mM NADP, 50 mM ADP, 10 μg hexokinase, and 10 mg of glucose-6-P dehydrogenase. The total volume in the cuvette was 1 ml. The reaction was followed at room temperature for 3 min.

In separate experiments, uniformly labeled glucose (1,2,3,4,5,6,6-D_7) was administered over 60 min in all three groups and followed by skeletal muscle excision *in situ*. Neutralized perchloric acid tissue extracts were run over a formate resin to isolate glyceraldehyde-3-phosphate (GAP). The eluted 2.5 M formate fraction containing GAP was evaporated to dryness and reacted with 55 μl of oxime reagent (30 mg hydroxylamine/ml pyridine) for 45 min at room temperature followed by the addition of 60 μl of TMS reagent [BSTFA + 10% (vol/vol) TMCS reagent (Pierce)] for 30 min at room. GAP labeling was determined by GC/MS (HP-5973) under electron impact ionization and selected ion monitoring (m/z 458–462). The ratio of GAP M+2 and M+3 to M+4 will provide an index of the relative exchange of the coupled GAPDH and PGK reactions caused by the redox reaction of GAPDH. GAP enrichments in the T_3-treated group were too low to be measured accurately and most likely are a result of the elevated lipid oxidation occurring in the skeletal muscle (substrate competition with glycolytic intermediates for oxidation).

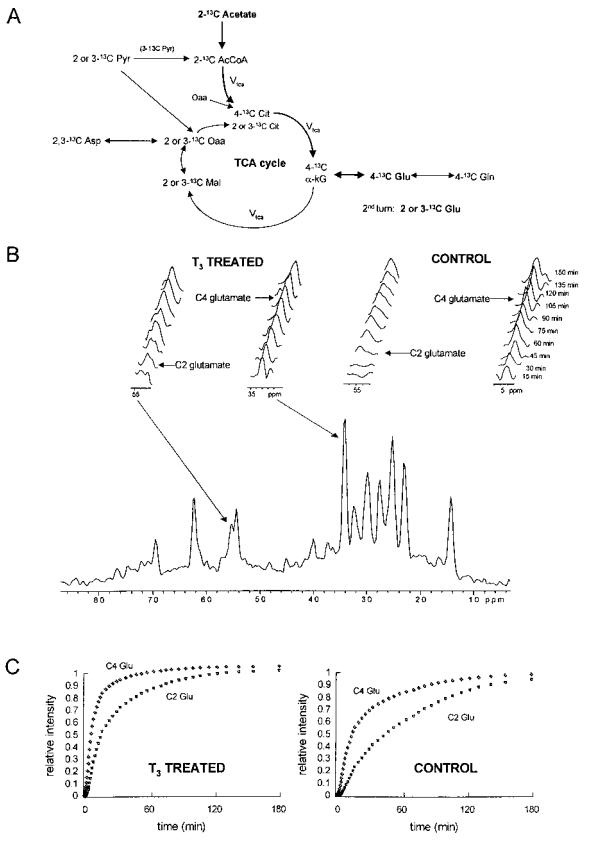

Fig. 1. ^{13}C NMR glutamate turnover study. (*A*) Intramuscular label flow schematic resulting from 2-^{13}C acetate administration (V_{tca}, TCA cycle flux). (*B*) A spectrum acquired from the rat hindlimb at 135–150 min is shown below. The 2-^{13}C glutamate peak appears at 55.5 ppm on the shoulder of the creatine/phosphocreatine peak (54.4 ppm), and the 4-^{13}C glutamate peak obscured by a coresonating aliphatic lipid peak appears at 34.4 ppm. Therefore, all spectra were baseline subtracted before peak integration. 3-^{13}C glutamate (27.9 ppm) and 2-^{13}C acetate (24.2 ppm) were not observed, because they reside in the frequency bandwidth that was partially suppressed because of the aliphatic lipid suppression pulse sequence used. Turnover of the 2- and 4-^{13}C glutamate peaks in the hindlimb muscles of control and T_3-treated rats is illustrated in the baseline subtracted spectra shown above. 2-^{13}C acetate label incorporates rapidly into 4-^{13}C glutamate and more slowly into 2-^{13}C glutamate (second turn of the TCA cycle). (*C*) The label turnover in 2- and 4-^{13}C glutamate was slower in the control vs. T_3-treated group as reflected by the representative turnover curves. $R^2 \geq 0.96$ ($n = 14$) for the best fit curves to the mathematical model.

Analytical Procedures. Glutamate (7) and acetate (8) ^{13}C enrichments in plasma and/or skeletal muscle tissue extracts were determined by GC/MS (HP-5971) under electron impact ionization. The P_i concentration was extrapolated from the baseline NMR spectrum by comparing peak integrals from P_i, γ-ATP, and measured ATP concentration (ATP assay kit no. 366; Sigma; modified for tissue analysis). Glutamate concentrations were measured with a 2700 Select analyzer (Yellow Springs Instruments).

Northern and Western Blot Analyses. Total RNA (30 μg) was electrophoresed in a 1.5% agarose gel containing formaldehyde

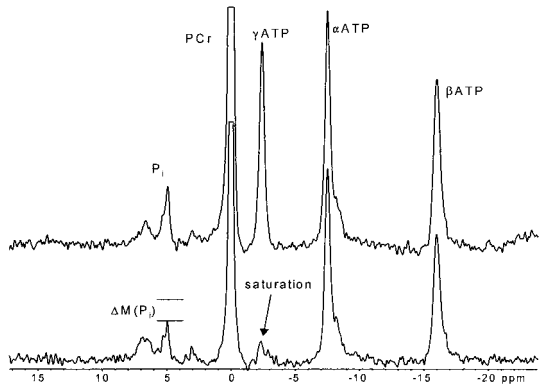

Fig. 2. ^{31}P NMR saturation transfer study. The spectra shown were obtained from a saturation transfer experiment performed in the hindlimb muscles of an awake rat. In the bottom spectrum, a continuous wave radio frequency pulse was used to saturate the γ-ATP resonance (-2.4 ppm). In the upper spectrum (no γ-ATP saturation), the continuous wave pulse frequency was placed symmetrically to the down-field side of P_i (4.9 ppm). The resulting loss in magnetization of P_i (ΔM) is due to the exchange of saturated γ-ATP nuclei with nonsaturated P_i nuclei.

as described by Lehrach *et al.* (9) and transferred to Hybond nylon membranes (Amersham Pharmacia) by capillary blotting. Probes were labeled by random priming with [α-^{32}P]dCTP (New England Nuclear) to a specific radioactivity of approximately 2×10^8 cpm/μg DNA. RNA blots were hybridized in hybridization buffer containing 50% (vol/vol) formamide, 0.25 M Na_2HPO_4, 0.25 M NaCl, and 1 mM EDTA at 65°C overnight and then washed in a solution containing 0.25 M Na_2HPO_4, 0.5% SDS, and 1 mM EDTA at 65°C for 20 min. Blots were exposed to scientific imaging film (New England Nuclear) at -80°C with intensifying screens. The signals on the membrane were quantified with an instant imager (Canberra, Meriden, CT).

Mitochondial protein (30 μg) after isolation was loaded on SDS/PAGE (4–15% Tris·HCl gradient gel from Bio-Rad) and transferred to nitrocellulose (Bio-Rad) at 100 V for 1 h. Nitrocellulose was then blocked in a buffer containing 5% (vol/vol) FBS in 1× TBS and 0.2% Tween 20 for 1 h at room temperature. The membrane was incubated with rabbit anti-human UCP3 antiserum (Alpha Diagnostic International, San Antonio, TX) at room temperature for 1 h. The membrane was then washed in 0.2% Tween 20 and 1× TBS for 10 min. After wash, the membrane was incubated with goat anti-rabbit IgG-horseradish peroxidase conjugate for 1 h at room temperature. The signal was detected by exposing the membrane with enhanced chemiluminescence on Hyperfilm ECL film (Amersham Pharmacia) and quantified by densitometry scanning.

Results and Discussion

Assessment of Tricarboxylic Acid (TCA) Cycle Substrate Oxidation by ^{13}C NMR. The TCA cycle generates reducing equivalents (NADH and $FADH_2$) that are necessary for mitochondrial respiration. Because the TCA cycle activity is coupled to O_2 consumption via a stoichiometric relationship with substrate use, the flux through the TCA cycle may be used as an index of substrate oxidation at steady state. Previously, ^{13}C NMR measurements of TCA cycle activity *in vivo* have been performed by observation of ^{13}C label turnover in glutamate, which reflects TCA cycle activity as a result of its equilibration with α-ketoglutarate (refs. 10–15; Fig. 1*A*). In this study, we measured ^{13}C label turnover in 4-^{13}C (34.4 ppm) and 2-^{13}C (55.5 ppm) glutamate (Fig. 1 *B* and *C*) in skeletal muscle during an i.v. infusion of 2-^{13}C acetate. The labeling of 4-^{13}C glutamate increases as a result of 2-^{13}C acetyl CoA condensing with oxaloacetate to produce 4-^{13}C citrate, which in turn labels 4-^{13}C α-ketoglutarate and 4-^{13}C glutamate (Fig. 1*A*). 2-^{13}C glutamate appeared more slowly than 4-^{13}C glutamate (Fig. 1 *B* and *C*) as a consequence of the additional turns of the TCA cycle, which are necessary to scramble the 4-^{13}C label of glutamate to 2- and 3-^{13}C glutamate (Fig. 1*A*). Steady-state isotopic enrichments in these metabolites were achieved between 120 and 150 min. Mathematical modeling of the TCA cycle flux was based on a nonlinear least squares fit (modified Levenberg–Marquardt process; minimum of 18,000 step intervals) of the calculated parameters (e.g., 4- and 2-^{13}C citrate, α-ketoglutarate, glutamate, etc.) derived from a set of isotopic mass balance equations that describe the label flow in associated pathways to the acquired NMR data (9–13). The best fit curves for 4-^{13}C glutamate and 2-^{13}C glutamate turnover in the control and T_3-treated groups are shown in Fig. 1*C*. The T_3 and DNP treatments resulted in ≈150% and ≈400% increases, respectively, in the TCA cycle flux relative to that in the control group (61 ± 21, 148 ± 25, and 310 ± 48 nmol/g per min in the control, T_3, and DNP groups, respectively; see Fig. 3*B*).

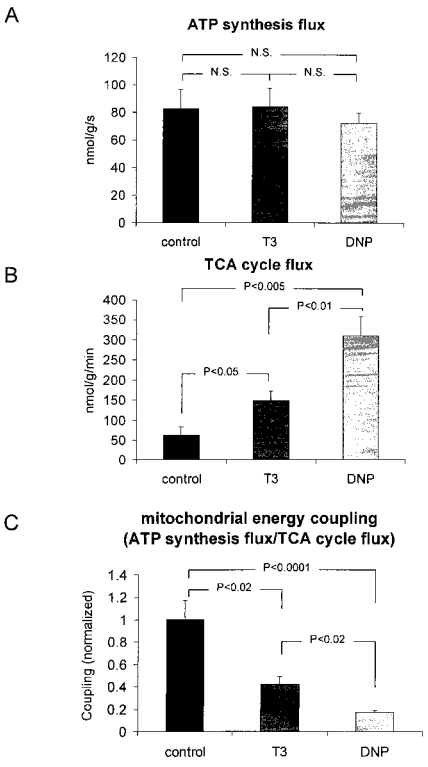

Fig. 3. Mitochondrial energy coupling measurements. (*A–C*) Data obtained from ^{13}C and ^{31}P NMR experiments in chronic T_3-treated and acute DNP-treated (known uncoupling agent) rats. (*A* and *B*) The calculated unidirectional ATP synthesis (*A*) and TCA cycle flux (*B*). There was a significant increase in TCA cycle flux in the T_3-treated vs. control group and a much greater increase in the DNP-treated rats. These data suggest that, although tissue viability was not compromised by the T_3 and DNP treatment as reflected by similar ATP synthesis flux in all three groups (*A*), there was a significantly increased rate of substrate oxidation required to generate the ATP (*B*). Therefore, when comparing the degree of coupling (normalized ratio of ATP synthesis flux to TCA cycle flux) between these two measurements (*C*), it is evident that there was significantly greater mitochondrial uncoupling occurring in the T_3 and DNP vs. control group. Data are presented as means ± SEM. N.S., not significant.

Assessment of ATP Production by ^{31}P NMR. Unidirectional ATP production was assessed noninvasively in rat skeletal muscle by using a ^{31}P saturation transfer method as initially described for

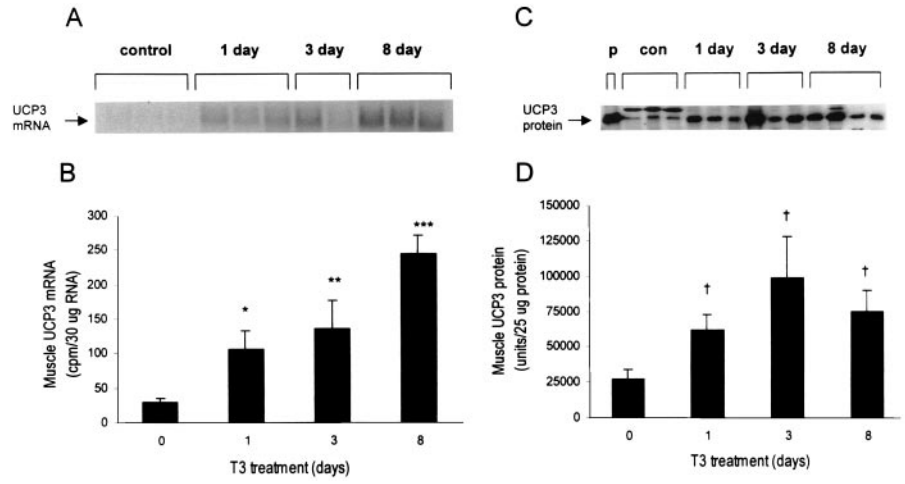

Fig. 4. UCP3 mRNA and protein measurements. (*A* and *B*) The Northern analysis for UCP3 mRNA in skeletal muscle reflects a graded increase in expression from 1 to 8 days of T_3 treatment vs. control. (*C* and *D*) The Western analysis for UCP3 protein in skeletal muscle reflects an immediate increase in UCP3 content after 1 day of T_3 treatment and no further increase thereafter. Data are presented as means ± SEM. p, purified protein; con, control; 1 day, 3 day, or 8 day, 1, 3, or 8 days of T_3 treatment. *, $P < 0.05$ vs. baseline; **, $P < 0.01$ vs. baseline; ***, $P < 0.0001$ vs. baseline; †, $P < 0.05$ vs. baseline.

measurements in *Escherichia coli* (16) and later in skeletal muscle (17). A saturation transfer experiment provides unique information with regard to unidirectional metabolic flux (see Alger and Shulman for review; ref. 18). In this procedure, the γ-ATP NMR peak is nulled with a saturating radio frequency pulse, and the reduction of the P_i peak as a result of the transfer of the saturated spins between γ-ATP and the P_i pool via F1F0 ATP_{ase} and other $P_i \rightarrow$ ATP pathways (e.g., GAPDH and PGK reactions) is monitored (Fig. 2). This decrease in magnetization of P_i (ΔM) may be used to determine the kinetics of ATP_{ase} activity once the glycolytic contributions of coupled GAPDH and PGK are accounted for. Although the net glycolytic contribution to the production of ATP (via GAPDH and PGK) vs. that of oxidative phosphorylation is small, these enzymes are at near equilibrium, and consequently, the unidirectional production of ATP (measured with the ^{31}P saturation transfer experiment) via these enzymes can be high. The rate constant (k) for $P_i \rightarrow$ ATP is defined by the following equation: $k = 1/T_{1app} \times \Delta M/M_0$, where T_{1app} is the longitudinal relaxation time of P_i during γ-ATP saturation and $\Delta M/M_0$ is the fractional change of the P_i magnetization during the saturation transfer experiment. Therefore, k may be calculated after acquiring spectra from the saturation transfer and inversion recovery experiments (see *Materials and Methods*). The unidirectional ATP synthesis flux ($P_i \rightarrow$ ATP) may be calculated as $k \times [P_i]$. In this procedure, there were no differences in the unidirectional ATP synthesis flux calculated for the control, T_3-treated, and DNP-treated groups (83 ± 14, 84 ± 14, and 73 ± 7 nmol/g per s, respectively; Fig. 3*A*).

To measure the degree of glycolytic contribution to these unidirectional ATP synthesis flux measurements, in separate experiments, uniformly labeled glucose (1,2,3,4,5,6,6-D_7) was administered, and measurements of GAP isotopomers were made. We were not able to detect any differences in relative exchange rates via the coupled GAPDH and PGK reactions in control vs. DNP-treated groups. It may be extrapolated from the measured unidirectional ATP synthesis flux and the deuterium exchange study described above that the ATP_{ase} flux in control and DNP-treated rats was the same. Additionally, direct measurements of ATP_{ase} activity in isolated mitochondria in the control and T_3-treated rats in this study were not different, suggesting that the skeletal muscle ATP_{ase} activity was similar under all three conditions in our study.

Assessment of Mitochondrial Energy Coupling Index (ATP Production/TCA Cycle Flux). The rates of ATP production were not altered by T_3 or DNP treatment as reflected by similar unidirectional ATP synthesis flux in all three groups (Fig. 3*A*). The fact that we did not measure a reduction in ATP synthesis flux after DNP treatment was most likely due to the administration of DNP well below the toxic threshold (4 mg/kg). To test whether we could measure a change in ATP synthesis flux, we administered 10–15 mg/kg DNP to a separate group of rats. This treatment resulted in a significant reduction of the measured $\Delta P_i/P_i$ (0.23 ± 0.05 vs. 0.13 ± 0.05 before and after DNP administration, respectively). These data suggest that at higher doses of DNP approaching toxic levels *in vivo*, ATP_{ase} function is decreased because of the reduction of the inner mitochondria membrane potential. In all three treatment groups, there was a substantial increase in the rate of substrate oxidation required to generate the same amount of ATP (Fig. 3*B*). The ratio of the measured unidirectional ATP synthesis flux to TCA cycle flux may be used as a qualitative index (if the measured unidirectional ATP synthesis flux and the glycolytic contribution to this measurement are equal in all groups) of the degree of coupling between mitochondrial substrate oxidation and ATP synthesis. The limitation of this analysis is that, if the measured ATP synthesis flux or glycolytic contribution to this flux were different between groups, then the glycolytic contribution would have to be subtracted from the overall ATP synthesis flux to obtain accurate ratios. Because we do not know the extent of basal mitochondrial uncoupling present as a result of combined proton transport and leaks across the inner mitochondrial membrane, this ratio was normalized to the control group (Fig. 3*C*).

When analyzed in this manner, it is evident that both T_3 and DNP treatments resulted in substantial decreases in mitochondrial energy coupling activity compared with than in the control group. The ≈60% decrease in mitochondrial energy coupling observed in the T_3-treated group correlated well with the 2- to 3-fold increase in UCP3 protein content in this group (Fig. 4*D*) and suggests that increased expression of UCP3 may be a mechanism by which thyroid hormone promotes increased energy use and thermogenesis *in vivo*, although we cannot rule out the possibility that the decreased mitochondrial energy coupling may be a consequence of increased proton permeability or increased function of other uncoupling protein isoforms. As a further validation of this NMR method, we were able to dem-

onstrate that treating rats with DNP, a well established protonophore and mitochondrial uncoupling agent, resulted in an even greater decrease in coupling (≈80%).

Obesity is becoming increasingly prevalent in Western civilizations as a consequence of a shift toward increased caloric consumption and a sedentary lifestyle (19). Approximately 55% of Americans are currently considered overweight (ref. 19; body mass index > 25), and obesity is known to be a major risk factor for both coronary heart disease and type 2 diabetes (non-insulin-dependent diabetes mellitus; ref. 20). There is therefore considerable interest in the recently discovered UCP3 protein as a potential target for treating obesity and type 2 diabetes. This *in vivo* NMR approach should therefore be a useful method for exploring the regulation of uncoupling protein activity in humans and elucidating its role in energy metabolism and obesity.

G.I.S. is an investigator for the Howard Hughes Medical Institute. This study was supported by United States Public Health Service Grants RO1 DK-40936 and P30 DK-45735, and B.M.J. was supported by a Mentor-Based Postdoctoral Fellowship from the American Diabetes Association.

1. Himms-Hagen, J. (1989) *Prog. Lipid Res.* **28,** 67–115.
2. Boss, O., Samec, S., Paoloni-Giacobino, A., Rossier, C., Dulloo, A., Seydoux, J., Muzzin, P. & Giacobino, J. P. (1997) *FEBS Lett.* **408,** 39–42.
3. Vidal-Puig, A., Solanes, G., Grujic, D., Flier, J. S. & Lowell, B. B. (1997) *Biochem. Biophys. Res. Commun.* **235,** 79–82.
4. Gong, D.-W., He, Y., Karas, M. & Reitman, M. (1997) *J. Biol. Chem.* **272,** 24129–24132.
5. Field, J., Beldings, H. S. & Martin, A. W. (1939) *J. Cell. Comp. Physiol.* **14,** 143–157.
6. Petersen, K. F., Cline, G. W., Blair, J. B. & Shulman, G. I. (1994) *Am. J. Physiol.* **30,** E273–E277.
7. Beylot, M., David, F. & Brunengraber, H. (1993) *Anal. Biochem.* **212,** 532–536.
8. Powers, L., Osborn, M. K., Yang, D., Kien, C. L., Murray, R. D., Beylot, M. & Brunengraber, H. (1995) *J. Mass Spectrom.* **30,** 747–754.
9. Lehrach, H., Frischauf, A. M. & Philipson, L. (1985) *Prog. Clin. Biol. Res.* **177,** 7–15.
10. Fitzpatrick, S. M., Hetherington, H. P., Behar, K. L. & Shulman, R. G. (1990) *J. Cereb. Blood Flow Metab.* **10,** 170–179.
11. Mason, G. F., Rothman, D. L., Behar, K. L. & Shulman, R. G. (1992) *J. Cereb. Blood Flow Metab.* **12,** 434–447.
12. Yu, X., White, L. T., Doumen, C., Damico, L. A., LaNoue, K. F., Alpert, N. M. & Lewandowski, E. D. (1995) *Biophys. J.* **69,** 2090–2102.
13. Chance, E. M., Seeholzer, S. H., Kobayashi, K. & Williamson, J. R. (1983) *J. Biol. Chem.* **258,** 13785–13794.
14. Jucker, B. M., Lee, J. Y. & Shulman, R. G. (1998) *J. Biol. Chem.* **273,** 12187–12194.
15. Szczepaniak, E. E., Babcock, L. S., Malloy, C. R. & Sherry, A. D. (1996) *Magn. Reson. Med.* **36,** 451–457.
16. Brown, T. R., Ugurbil, K. & Shulman, R. G. (1977) *Proc. Natl. Acad. Sci. USA* **74,** 5551–5553.
17. Brindle, K. M., Blackledge, M. J., Challiss, R. A. J. & Radda, G. K. (1989) *Biochemistry* **28,** 4887–4893.
18. Alger, J. R. & Shulman, R. G. (1984) *Q. Rev. Biophys.* **17,** 83–124.
19. Flegal, K. M., Carroll, M. D., Kuczmarski, R. J. & Johnson, C. L. (1998) *Int. J. Obes. Relat. Metab. Disord.* **22,** 39–47.
20. James, W. P. T. (1998) *Exp. Clin. Endocrinol. Diabetes* **106,** S1–S6.